Graphite Carbon Foam Films Prepared from Porous Polyimide with *In Situ* Formed Catalytic Nickel Particles

Yanling Luo, Qingyun Chen, Dan Zhu, Masaru Matsuo

Faculty of Human Life and Environment, Department of Textile and Apparel Science, Nara Women's University, Nara 630-8263, Japan

Received 11 December 2008; accepted 8 November 2009
DOI 10.1002/app.31764
Published online 7 January 2010 in Wiley InterScience (www.interscience.wiley.com).

ABSTRACT: This article describes the preparation of porous polyimide composites and carbon foam films with uniform and controllable porous structures, using nickel oleate as a pore-forming agent and as a precursor for catalyst formation for the carbonization process. Pore formation occurs by a phase separation initially producing a dispersion of nickel oleate liquid in the polyamide acid film. Subsequent heat treatment induces decomposition of the nickel oleate accompanied by the evolution of foam forming gas. Small nickel particles, formed by the decomposition of nickel oleate, melt as the process temperature rises above 1200°C and these molten nickel particles then play an important catalytic role in promoting the graphitization of the polyimide composites as part of a dynamic process forming pores proceeding through the thickness of the film. These porous structures are maintained after the removal of the nickel by pyrolysis. The thermal behavior and structure of the porous polyimide films were examined and the porosity and stacking structures of the carbon foam films formed by polyimide pyrolysis were investigated. The results indicate that the pore size of the carbon foams could be controlled over a broad range by varying the nickel oleate content participating in the polymerization reaction. © 2010 Wiley Periodicals, Inc. J Appl Polym Sci 116: 2110–2118, 2010

Key words: foams; polyimides; morphology; macroporous polymers; carbonization

INTRODUCTION

Carbon foams are defined as having a total porosity greater than 45%.[1–3] They have been used in many applications such as heat exchangers, catalyst supports, gas absorbents, and filtration or separation devices.[4,5] To obtain these porous materials, a number of techniques have been reported including use of blowing agents,[6] phase inversion of cast films,[7,8] microwave processing, the use of self-organizing systems as templates,[9–11] and pyrolysis of thermally labile phase-separated compounds.[12,13] Pyrolysis of polymeric precursors, in particular, is a widely used method for the production of carbon foam films, because the method is straightforward in operation and allows control of the pore structure in the film product.

A number of polyimide-labile polymer blends have been reported as porous carbon precursors. For example, blends of poly(4,4′-oxydiphenylene pyromellitimide) with poly(methyl methacrylate) were used to prepare a macroporous film, and poly(*para*-phenylene pyromellitimide)/poly(ethylene glycol) blends were used to prepare porous carbon materials.[14] Pore formation from such polymer blends is due to a phase separation mechanism, limiting the choice of blend components to suitably phase separating mixtures. Unlike the blending method, the use of long alkyl chain fatty acids as pore-forming agents is not limited by blend composition, due to the being readily soluble property of these materials in organic solvents and also being immiscible with polyimide. In addition, low cost makes fatty acids competitive as agents for preparation of porous materials.

Nickel ultrafine particles are known to be more catalytically active in carbonization process than presynthesized nickel catalysts.[15] However, the general method of producing nano-nickel particles is technically challenging, and may require the use of $Ni(CO)_4$, which is a highly hazardous material and is consequently no longer commercially available. Nickel formate or nickel stearate are both regarded as superior precursors for producing metallic nickel. In previous studies by Puntes et al.[16] and Sun et al.,[17] oleic acid was used to disperse the nickel particles because of the good solubility of the metal oleate in organic solvents, and the dispersion was used to produce magnetic nanocrystals via the decomposition of organometallic precursors.

In this article, 3,3′,4,4′-benzophenone tetracarboxylic dianhydride (BTDA) based polyimide with a

Correspondence to: M. Matsuo (m-matsuo@cc.nara-wu.ac.jp).

flexible ketone (—CO—) bridging group was used as the precursor to produce carbon films.

The carbonization behavior of BTDA based polyimide has been rarely studied because of the relative difficulty in obtaining satisfactory yields of graphite carbon compared with Kapton polyimide. In this study, BTDA based polyimide is used to prepare porous graphitic films and porous carbon films with turbostratic (quasi-graphitic) structure, catalyzed by nickel particles. Nickel oleate was prepared by saponification and extraction from Ni^{2+} aqueous solution, and polyimide/nickel composites were prepared *in situ* by polymerization in *n*-methyl-2-pyrrolidone (NMP) solution. Nickel particles were formed by thermal decomposition of nickel oleate in the polymer films, and the associated evolution of gaseous decomposition products was used to prepare polyimide foam films. Carbon foams with uniform and controllable porous structures were prepared by nickel-catalyzed carbonization of porous polyimide films. The carbon foam films prepared from BTDA based polyimide with flexible ketone (—CO—) bridging groups provided a high degree of carbonization.

EXPERIMENTAL

Chemicals

4,4′-oxydianiline (ODA) and 3,3′,4,4′-benzophenone tetracarboxylic dianhydride (BTDA) were purchased from Tokyo Chemical Industry Co., Japan. The ODA and BTDA were dried under vacuum for 10 h at 150°C before polymerization. NMP was purchased from Nacalai Tesque, Kyoto, Japan, and was dried by molecular sieve for 3 days. Oleic acid and nickel (II) formate dihydrate were purchased from Wako Pure Chemical Industries, Japan.

Preparation of nickel oleate

The pH of 100 mL of an aqueous solution of 0.2 mol L^{-1} Ni $(HCOO)_2 \cdot 2H_2O$ was adjusted to 8.0–9.0 with dilute NaOH. Sufficient oleic acid $C_{17}H_{34}COOH$ was added to adjust the mole ratio of oleic acid to Ni^{2+} to 1.2 : 1, whereupon the mixture was allowed to settle into two layers. The upper (oil) layer was composed of oleic acid, whereas the lower layer was aqueous $Ni(HCOO)_2$. The mixture was stirred for about 4 h at 120°C until the oil layer became green in color, and the aqueous phase became transparent with an appreciably green color. The mixture was separated using a separating funnel and the oil phase collected and dried in a vacuum oven to remove water. The oil phase was then characterized by FTIR spectroscopy. The FTIR confirmed that the oil phase was composed of nickel oleate. The Ni weight fraction (7.4%) in the prepared nickel oleate was determined by thermogravimetric (TG) analysis, as shown in Figure 5(a).

Preparation of the polyimide/nickel composite

The polyamide acid-nickel oleate composites were synthesized by an *in situ* polymerization method.[18,19] In a typical synthesis, ODA (1.0 g) was mixed with an appropriate amount of NMP solvent under an N_2 atmosphere. After complete dissolution of ODA, nickel oleate (1.26 g) was added, and then BTDA (1.62 g) was added to the mixture in three aliquots at 30 min intervals. After stirring the mixture for a further 12 h at room temperature, a golden yellow nickel oleate/polyamide acid solution was obtained.

The precursor solution of polyamide acid and nickel oleate in NMP was cast on a glass plate and cured by heating under an N_2 atmosphere for about 4 h at 70°C until a cured film was formed. The film was heated gradually to remove the NMP and to promote imidization. Heating was carried out in four stages: 100°C, 1 h; 150°C, 1 h; 250°C, 1 h; 300°C, 2 h. The polyimide/nickel composite film was then cooled to room temperature. The Ni oleate content was calculated by using the mass of added Ni oleate and the total mass of admixture participating in the reaction (BTDA, ODA, and Ni oleate). The nickel content in the polyimide/nickel composite was calculated by the nickel mass fraction of the added nickel oleate and the resultant polyimide composite.

In this research, polyimide composites with Ni weight fractions of 2%, 5%, and 7% were prepared, in which the corresponding contents of Ni oleate ($Ni(C_{17}H_{34}COO)_2$) against the admixture participated in reaction (BTDA, ODA, and Ni oleate) were 17%, 33%, and 40%, respectively. The calculation process is as follows:

The content of Ni oleate (X) is given approximately as the weight fraction by the equation as follows:

$$X = \frac{M_o}{M_T} \times 100\%$$

where M_o is the mass of nickel oleate participating in the reaction, and M_T is the total mass of admixture participating in the reaction (BTDA, ODA, and Ni oleate).

The mass of nickel, P, is calculated on the basis of the mass of nickel oleate participating in the reaction, M_o, and the weight fraction of nickel in nickel oleate determined by TG analysis as shown in Figure 5(a), 7.4%. That is, the mass of nickel, P, is given as, $P = M_o \times 7.4\%$. Then the weight fraction of nickel in polyimide composite, Y, is given as follows:

$$Y = \frac{P}{W} \times 100\%$$

where W is the mass of resultant polyimide/nickel composite film.

Thus, the nickel weight fraction refers to the weight fraction of nickel within the polyimide/nickel specimen before pyrolysis. Specimens were prepared with three different amounts of Ni oleate and a constant amount of BTDA and ODA in the admixture as previously discussed.

Carbonization of the polyimide films

The polyimide/nickel composite films were cut into pieces, sandwiched between graphite plates and heated to 1600°C at an optimized heating rate of 6.7°C min^{-1},[20,21] and then kept at that temperature for 2 h or 5 h under a flowing argon atmosphere. Black carbon films were obtained after cooling to room temperature. The thickness of resultant carbon film was determined by scanning electron microscope (SEM) examination. As will be discussed in detail later, the SEM and energy dispersive X-ray spectroscopy (EDS) analyses on cross sections of the carbon films show that there are no nickel particles in the cross section, because the high density molten nickel has migrated to the bottom surface of the film during the high temperature heat treatment.

SEM examination of the carbon films prepared by pyrolysis of polyimide composite with 5% nickel was used to determine the achieved thicknesses at 68 μm, 64.8 μm, and 63 μm for heat treatments at 900°C, 1200°C, and 1600°C, respectively. A slight decrease in thickness occurred with increasing temperature associated with an increase in degree of graphitization.

TG analysis of the polyimide composites was carried out using a TG/DTA 6300 (SII Nano Technology) instrument at 10°C min^{-1} heating rate under a nitrogen atmosphere. Wide angle X-ray diffraction (WAXD) was performed with a 12 kW rotating-anode X-ray generator (Rigaku RDA-rA) operated at 150 mA and 40 kV. The CuKα radiation beam was monochromatized with a plate-like graphite monochromator. The X-ray beam was orientated to be perpendicular to the film surface to obtain the diffraction peaks from the graphite and nickel crystallites.

Samples for FTIR spectroscopy were prepared by spreading the precursor solution onto a KBr tablet. The KBr tablet was then heated, using the same temperature/time schedule used in the preparation of the composites, and spectra were taken at intervals to determine the spectral changes associated with imidization of the precursor solution. The FTIR measurements were performed in the 400–4000 cm^{-1} range at 2 cm^{-1} resolution. Twenty scans were averaged for each spectrum.

Scanning electron microscopy (SEM) and EDS were conducted using a JSM-6700F field emission scanning electron microscope and a JSM-B300 (JEOL Co.) instrument.

Nitrogen adsorption and desorption isotherms were performed with a Belsorp-mini instrument from Bel Japan.

RESULTS AND DISCUSSION

Formation of the porous morphology

From the analysis of our experimental results, a schematic diagram is proposed for the process to describe the formation of macropores in the polyimide film and resultant graphitic carbon films.

Figure 1 shows the proposed process for the formation of pores in polyimide films and carbon films. The precursor solution containing nickel oleate and polyamide acid was heated for 4 h in nitrogen at 70°C to gradually remove the NMP. This heating process led to the separation of the polyamide acid and nickel oleate liquid phases. After 4 h, most of the NMP was removed, and a cured polyamide acid film was formed containing the dispersed nickel

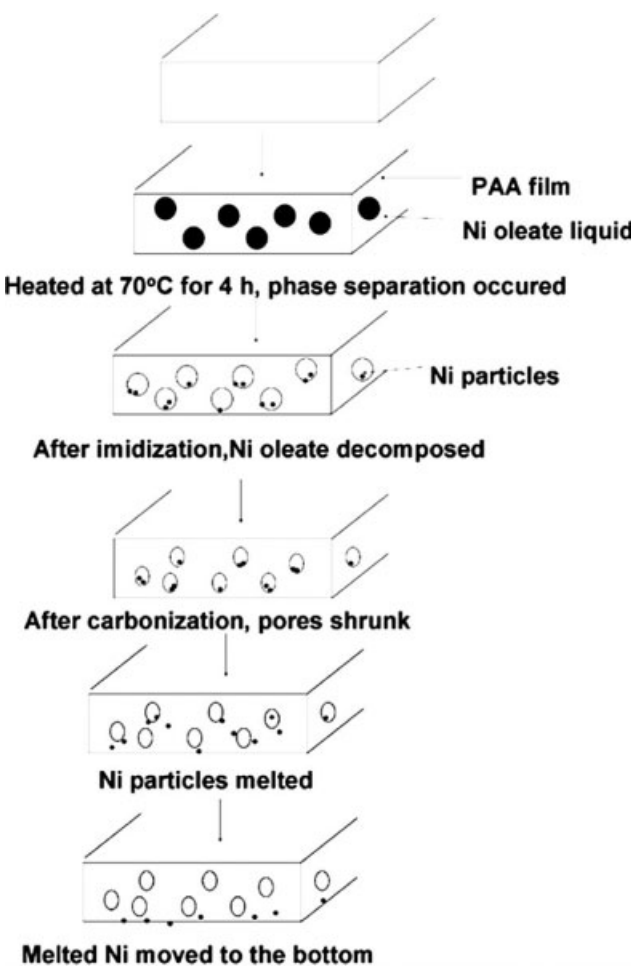

Figure 1 Schematic illustration for formation of macropores in polyimide films and carbon films.

oleate liquid phase. This separation is proposed as the cause of the formation of macropores occupied by liquid nickel oleate. In the subsequent imidization process, the nickel oleate decomposed and released gas species such as CO and CO_2 leaving gas-filled void spaces in the film.[22] Monodispersed magnetic metal nanoparticles were produced in the void spaces.[22] TG analysis of the nickel oleate indicated that this decomposition starts at $\sim$ 150°C, and the evolution of this gas leaves voids which had been formerly occupied by nickel oleate liquid in the polymer matrix. As the process temperature increases, imidization occurs accompanied by a complete removal of residual NMP and polyimide film was obtained. The thermal decomposition of nickel oleate can be represented by the following equation:

$$\mathrm{Ni(C_{17}H_{34}COO)_2} \xrightarrow{\Delta} \mathrm{Ni(or\ NiO)} + \text{gaseous species } (\mathrm{H_2, CO, CO_2, H_2O})$$

After decomposition of Ni oleate, some nickel particles remain in the pores. During the carbonization process of polyimide, the temperature increases up to the melting point of nickel and the dense molten nickel flows gradually from the pores down to the bottom surface of the film. During this process, the molten nickel plays an important role as a catalyst to accelerate graphitization. This catalytic effect has been reported elsewhere.[15] Unfortunately, as discussed later, we could not observe the nickel particles in the polyimide film by SEM due to the low conductivity of polyimide matrix.

FTIR spectroscopy study

The spectrum of oleic acid in Figure 2(a) shows a strong C=O stretch band at about 1710 cm^{-1}. Weak bands associated with scissor and bending vibrations of —CH_2— and CH—CO groups appear at 1476 cm^{-1} and 1415 cm^{-1}, respectively. The strong absorptions at 2853 cm^{-1} and 2925 cm^{-1} can be attributed to methylene and methyl symmetric stretching vibrations, respectively. In the spectrum of the Ni oleate, a band appears at about 1615 cm^{-1}, indicating complexation between the carboxylate and Ni^{2+}. There is no other band shifts relative to the spectrum of oleic acid, indicating that Ni^{2+} binds only to carboxylate. The band at 1710 cm^{-1} still appears in the Ni oleate spectrum, indicating that some free oleic acid residue was present in the Ni oleate sample.

The FTIR spectra of polyimide films recorded at different stages of curing are shown in Figure 2(b). The intensity of the imide carbonyl absorption at 1383 cm^{-1} proves that the curing process converted polyamide acid to polyimide. With increase in curing temperature, the intensity of this band increases,

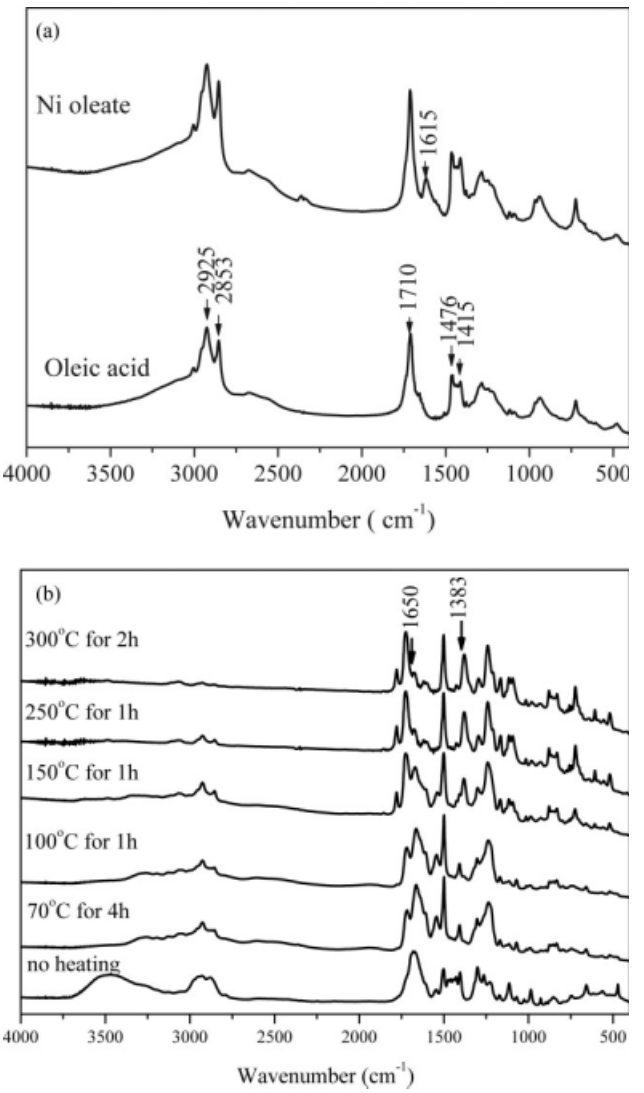

Figure 2 FTIR spectra of (a) oleic acid and nickel oleate, (b) polyamide acid and nickel oleate samples cured at the indicated condition.

indicating an increasing degree of imidization, whereas the C=O band at 1650 cm^{-1} for polyamide acid gradually decreases in intensity. After heating the composite for 1 h at 250°C, the imide carbonyl band showed no change in intensity, indicating that imidization of polyamide acid was complete. The subsequent heat treatment at 300°C was performed to promote volatilization of oleic acid.

Scanning electron microscopy (SEM)

SEM observation was used to investigate the structure of the polyimide foam materials and carbon films obtained by pyrolysis. The images in Figure 3 clearly show the presence of macropores in the cross section of polyimide films and carbon films. The average size of the pores was reduced and the pores appeared to be relatively uniform and regular in

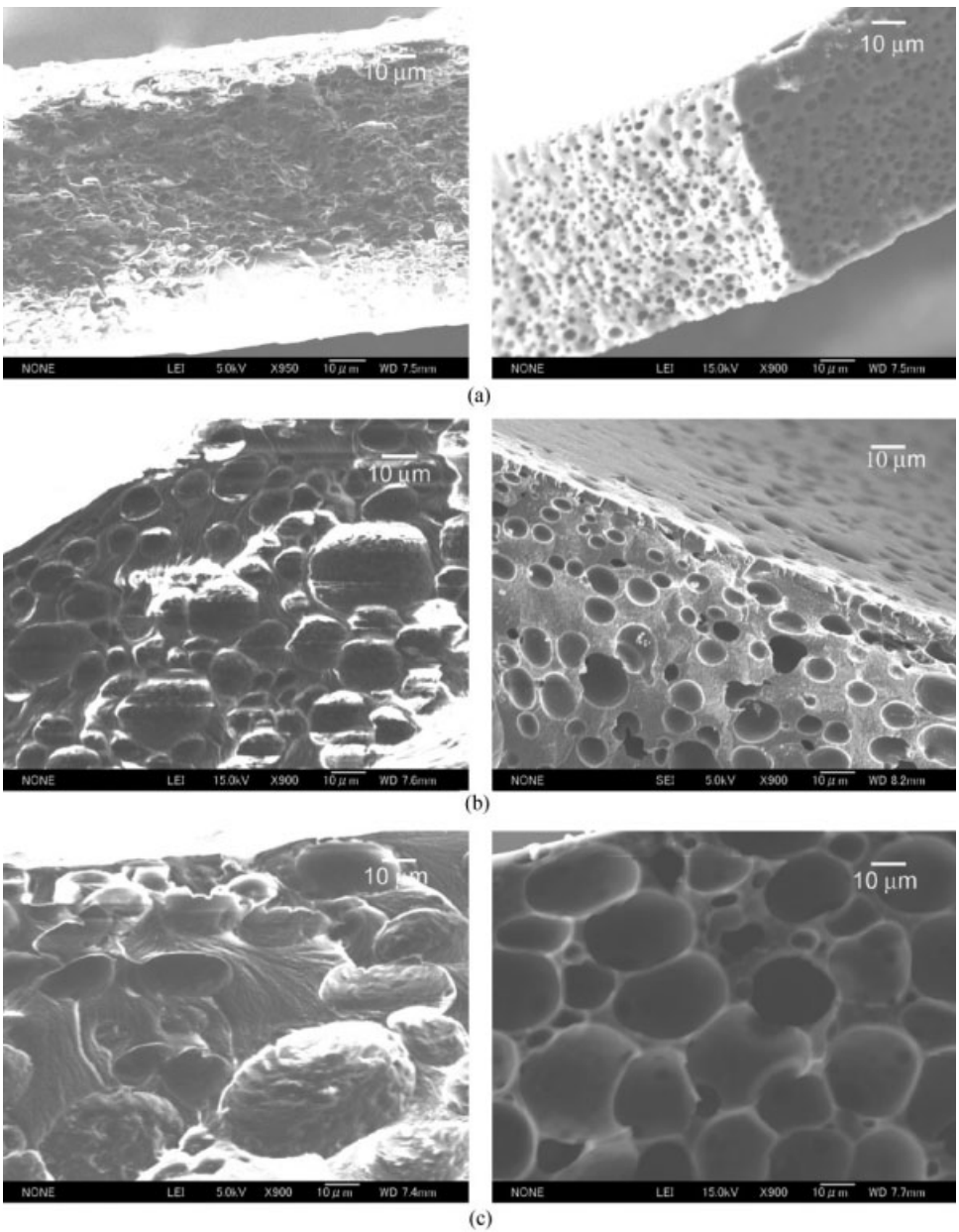

Figure 3 SEM images of the cross section for polyimide composite films and carbon films prepared by different contents of Ni oleate (a) 17% (ca. 2% Ni), (b) 33% (ca. 5% Ni), and (c) 40% (ca. 7% Ni).

shape after carbonization. The size distribution of the macropores in the carbon films was determined by observation of about 150 pores in SEM images of film cross sections (see Fig. 4). The pore size increased from 2.1 to 25.9 μm with an increase in the Ni oleate content, indicating that the macropore size can be controlled over a broad range by varying the proportion of Ni oleate. In addition, the walls between pores became thinner as pore size increased.

Thermogravimetric study

Figure 5(a) shows the TG and the first derivative TG (DTG) curves for a nickel oleate. The curves indicate that the Ni oleate starts to decompose at about 150°C, the associated gas evolution forms pores in the polymer matrix film as shown in Figure 1. There are two peaks in the DTG curve corresponding to the two mass losses in the TGA curve. The first peak appears at about 265°C, which is due to the decomposition of oleic acid. The second weight loss at about 350°C, which is due to the decomposition of NiO.

Assuming that the nickel oleate decomposed completely in the TG analysis, the residual mass can be obtained from the TG curve, as previously discussed, and the 7.4% value obtained, corresponds to the mass of Ni. The value is slightly less than the

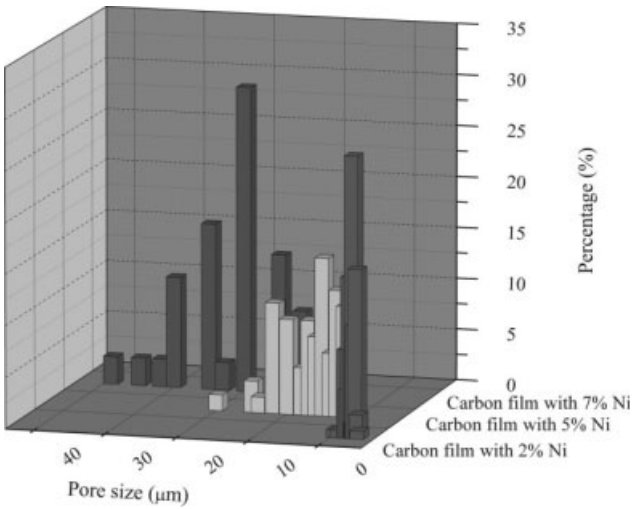

Figure 4 Pore size distribution of porous carbon films prepared by pyrolysis of polyimide composite films with various nickel content.

proportion by weight of nickel (9.2%) in the nickel oleate, which is calculated from the assumed chemical formula $Ni(C_{17}H_{33}COO)_2$. The small discrepancy between the nickel content obtained from the residual mass of TG analysis and the calculated content by the chemical formula may be due to the fact that in the preparation of nickel oleate the extraction of Ni^{2+} by oleic acid from Ni^{2+} aqueous solution is a reversible process. This means that the nickel in aqueous $Ni(HCOO)_2$ did not completely convert into nickel oleate.

The thermal behavior of polyimide/nickel composites is shown in Figure 5(b). The nickel filled polyimide composite film exhibited good heat resistance. However, the decomposition temperature shifted to slightly a lower temperature with increasing nickel content, indicating that the heat resistance of the polyimide composite decreased with increasing nickel content. The reason is probably due to the catalytic effect of the nickel, which played an important role in alkane dehydrogenation. Undecomposed residue of polyimide is still present at 800°C. The yield of polyimide residue decreased with the increase of nickel content in polyimide matrix, which is probably due to the nickel accelerating the catalytic decomposition of polyimide.

The DTG curves of the polyimide/nickel composites are shown in Figure 5(c). The first peak appearing at about 200°C is due to the decomposition of the small amount of residual oleic acid in the polyimide composite films after the heat treatment process. The specific weight losses from the TG results were 0%, 2.7%, and 3.9% for polyimide composites with 2%, 5%, and 7% Ni, respectively. Accordingly, the peak for the polyimide composite with 2% nickel did not appear at 200°C in the DTG curve, indicating that oleic acid had been removed completely from the composite by the heat treatment.

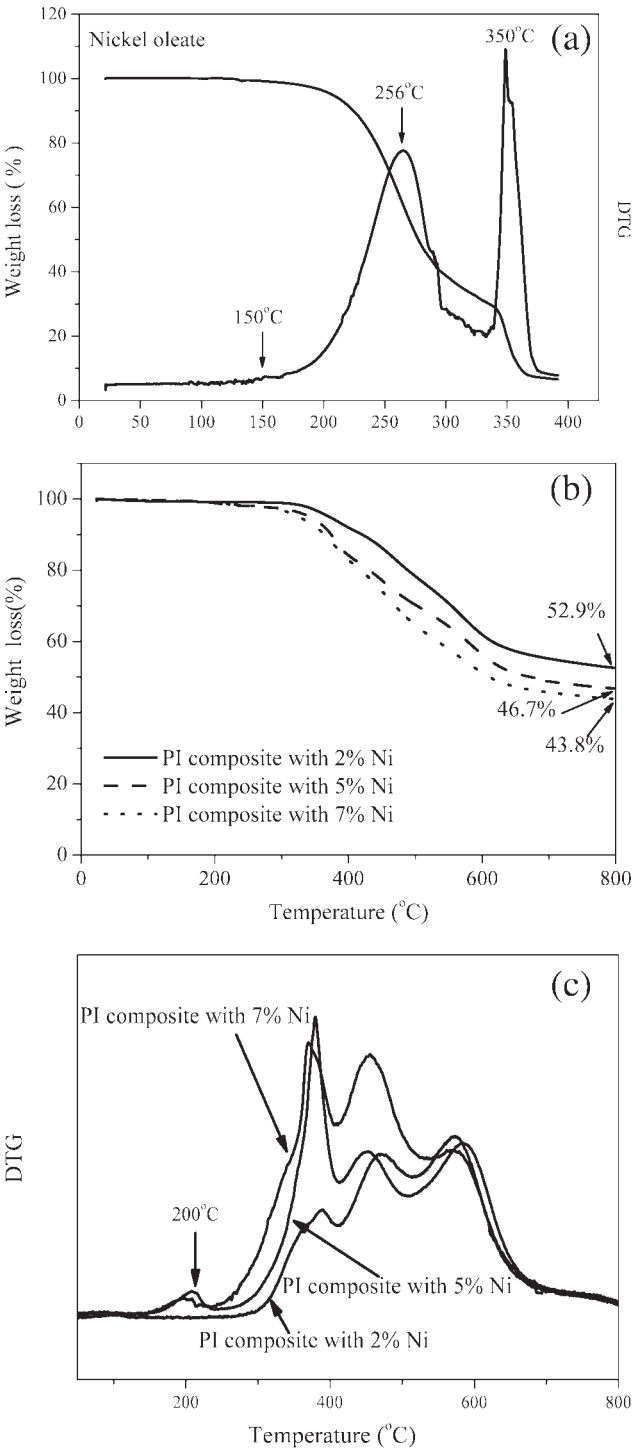

Figure 5 (a) TG and DTG curves for nickel oleate, (b) TG analysis for polyimide/nickel composite, and (c) DTG analysis for polyimide/nickel composite.

The second mass loss at 400°C corresponds to the decomposition of Ni oleate,[23] which leads to the formation of ferromagnetic Ni nanoparticles[24] that are incorporated in the polymer. The temperature corresponding to the third peak is about 471°C, 456°C,

and 451°C for the composites with 2%, 5%, and 7% nickel, respectively. This weight loss can be attributed to the decomposition of the imide ring, which produces CO_2 and CO, and the weight loss above 600°C, as shown in Figure 5(b), is due to loss of H_2.[25,26]

Wide angle X-ray diffraction

After the pyrolysis of the porous polyimide composite at 900°C, the (002) reflection shows a broad peak [Fig. 6(a)], indicating that the porous carbon was composed of an amorphous carbon structure with highly disordered graphene sheets. By contrast, the carbon prepared at 1200°C had a graphitic structure. The (002) reflection is at 26.2° and the (10) reflection from the porous graphite framework appears at 43°, in addition to the reflection from nickel crystallites. For carbon film prepared by heat treatment at 1600°C, the intensity from the (002) reflection did not change, whereas the Ni (111) reflection had reduced intensity. This is due to the fact that most of the high density melted Ni particles migrated to the bottom of the film under the carbonization process and very few particles were discovered in the cross section irradiated by X-ray beam. Nickel performed as a catalyst to promote the carbonization process. The lattice spacing for the (002) plane was 0.345 nm for the specimen heated at 1600°C, which is slightly larger than for perfect graphite (0.3354 nm), indicating imperfect graphitic carbon with turbostratic structure.

Figure 6(b) displays the influence of nickel content on the degree of graphitization. The (002) reflection became more intense and more narrow with increase in the proportion of Ni. According to the catalytic mechanism which involves dissolution of amorphous carbon in metal catalyst,[27–29] carbon atoms formed an epitaxial graphite monolayer on the (111) plane of Ni crystallites.[29] During the heating period, graphitization starts on the surface of nickel particles as proposed by Lamber et al.[29] The polyimide matrix in contact with nickel particles tended to be converted to the turbostratic graphitic structure. The yield of the turbostratic structure increased with increasing nickel content.

The similar profiles of the (002) reflections of the carbon films prepared by heating at 1600°C for 2 and 5 h [Fig. 6(b)] suggest that prolongation of the heating period did not increase the extent of carbonization.

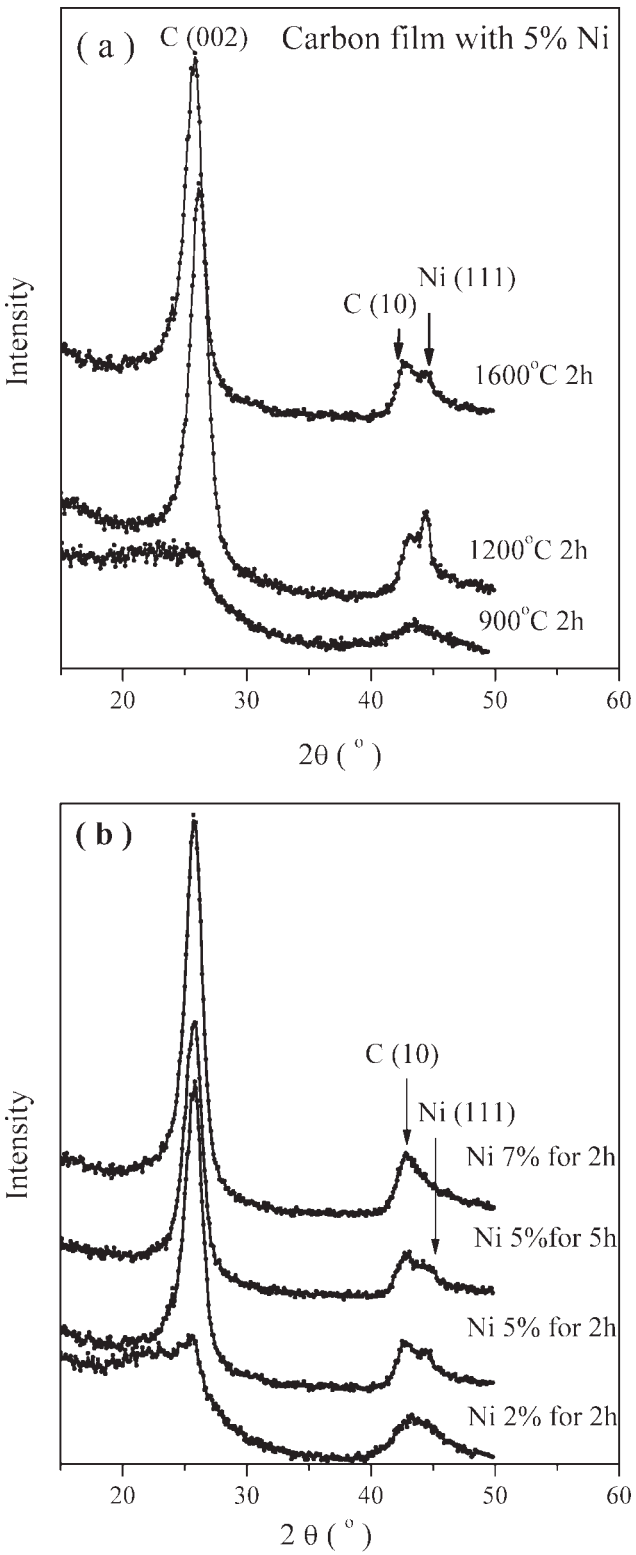

Figure 6 WAXD curves for porous carbon films prepared from: (a) the composite containing about 5% nickel heat-treated at different temperature, (b) the composite with different Ni content heat-treated at 1600°C for 2 h or 5 h.

Energy dispersive X-ray spectroscopy

Figure 7(a–c) shows the EDS spectra and SEM images for the cross section and upper and bottom surfaces. The examination was carried out to

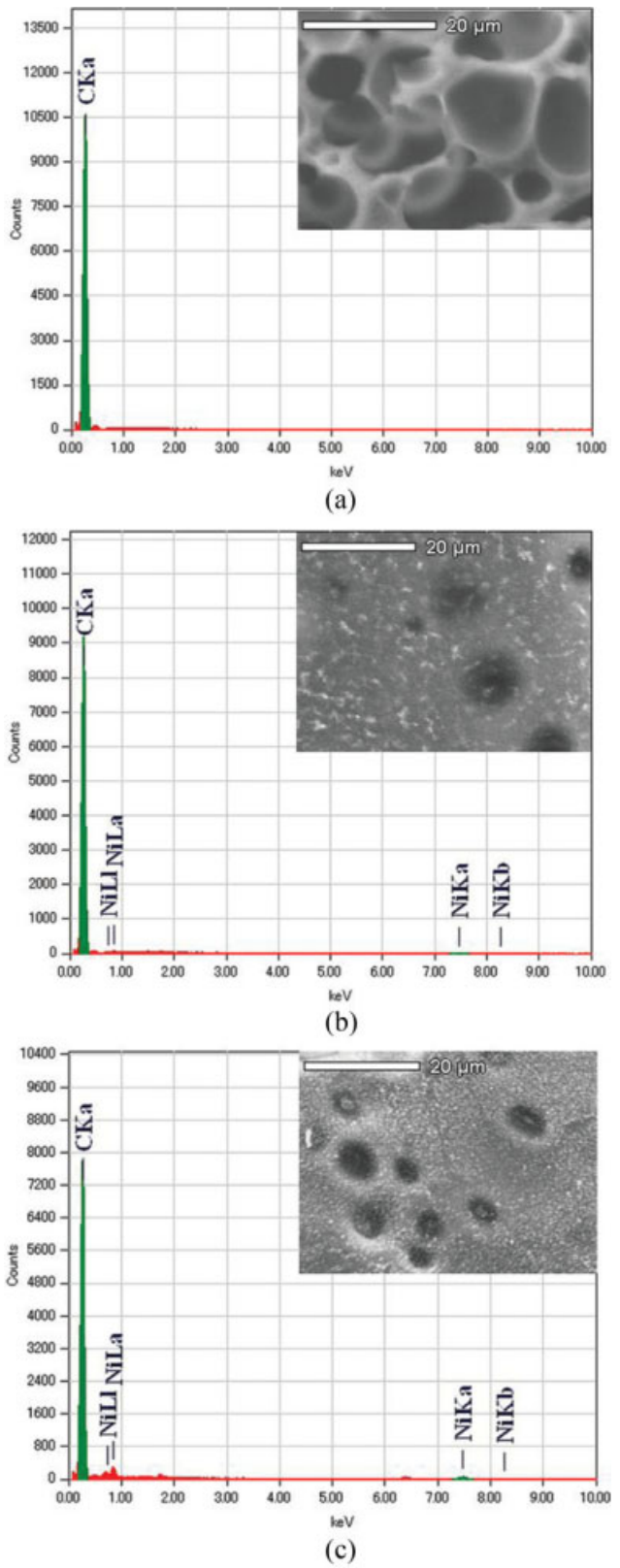

Figure 7 EDS spectra of (a) the cross section, (b) the upper surface, and (c) the bottom surface of the carbon film obtained from polyimide composite filled with 5% nickel. [Color figure can be viewed in the online issue, which is available at www.interscience.wiley.com.]

confirm that the nickel crystallites indicated by the WAXD measurement, were present at the bottom surface. This migration was attributed to flowing of molten nickel during the 1600°C carbonization process. The spectrum for the cross section shows a peak associated with carbon element and the spectrum for the upper surface shows very small nickel element peak. In contrast, the spectrum for the bottom surface shows significant nickel element content. These observations confirm that the nickel element in the cross section (molten at by 1600°C) has migrated to the lower surface, an observation which is in good agreement with the WAXD results. The EDS spectra are also consistent with our supposition regarding the mechanism for the formation of the pores (Fig. 1), whereby the decomposition of the Ni oleate forms gases which produce the porous morphology. Consequently, Ni particle residues were left in the pores. The peak intensity of carbon element in the cross section is higher than the carbon peak intensity at the surface, which indicates that the degree of graphitization was higher in the middle of the cross section compared with the surface. Thus, it is demonstrated that most of the nickel particles were initially dispersed in the pores according to the solution-precipitation mechanism before the carbonization at 1600°C.[27,29] It should be noted that the nickel particles could not be observed by high powered SEM because of the low conductivity of polyimide matrix.

Adsorption measurements

Nitrogen sorption and desorption experiments were performed to study surface properties of the polyimide composites and the carbon films. The adsorption experiments were carried out at liquid nitrogen temperatures. In Figure 8, p is the measured equilibrium pressure, and p_0 is the vapor pressure of nitrogen at the temperature of the measurement. This figure shows that for every sample, an open hysteresis loop was obtained down to low pressures, which may indicate swelling of the adsorbent during the adsorption process or from physical adsorption accompanied to some extent by chemisorption.[30]

The amount of adsorbed volume increased gradually as the relative pressure increased, and the adsorption curves showed a convex shape in the whole pressure range, which can be attributed to a Type III absorption isotherm.[31] Thus, the interaction between the nitrogen and the samples was weak, and the monolayer density tended to be uneven on the adsorbent surface with a relatively high concentration of molecules located in the most active areas.[30] The measured adsorption capacity at $p/p_0 = 1$ was 102.01 $m^2\ g^{-1}$ for the carbon foam films obtained from the polyimide/2% Ni composite, and

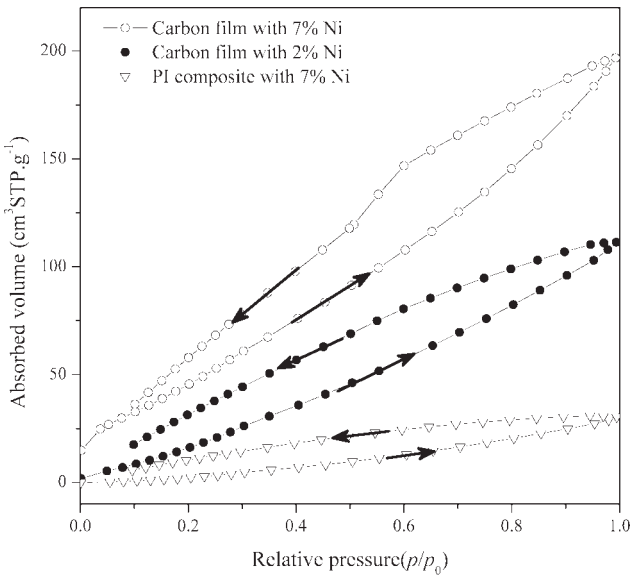

Figure 8 Nitrogen sorption isotherms of the indicated samples.

195.06 m^2 g^{-1} for the carbon foam films was obtained from the composite with 7% Ni. The 7% Ni doped polyimide composite and the corresponding carbon film obtained by carbonization had similar hysteresis shape, suggesting that different adsorbent surfaces had little influence on nitrogen adsorption.[32] However, the amount adsorbed increased after carbonization, which may arise from a different structure of the adsorbent surface or increase of the surface area after carbonization.

CONCLUSIONS

Preparation of porous carbon films with a high graphitic content was achieved by a straightforward procedure. Polyimide film filled with nickel particles was prepared by *in situ* polymerization of the polyimide monomers and Ni oleate, and the resultant polyimide composite was heat treated at 1600°C to give graphitic carbon foam films. The results indicate that nickel formed by thermal decomposition of nickel oleate played an important role as a very active catalyst for growing graphitic carbon foam. Carbon foam films with a high degree of graphitization could be prepared by mild thermal treatment at relatively low temperature under argon, and the pore size and structure could be controlled by varying the Ni oleate content participating in the reaction.

References

1. Aubert, J. H.; Sylwester, A. P. J Mater Sci 1991, 26, 5741.
2. Lee, J.; Sohn, K.; Hyeon, T. J Am Chem Soc 2001, 123, 5146.
3. Pekala, R. W.; Hopper, R. W. J Mater Sci 1987, 22, 1840.
4. Nakanishi, K. M.; Soga, N.; Tanaka, N. J Sol-Gel Sci Technol 1998, 13, 163.
5. Sarrade, S. J.; Rios, G. M.; Carles, M. Sep Purif Technol 1998, 14, 19.
6. Krause, B.; Diekmann, K.; Vandervegt, N. F. A.; Wessling, M. Macromolecules 2002, 35, 1738.
7. Echigo, Y.; Iwaya, Y.; Saito, M.; Tomioka, I. Macromolecules 1995, 28, 6684.
8. Shimizu, H.; Kawakam, H.; Nagaoka, S. Polym Adv Technol 2002, 13, 370.
9. Huck, W. T. S.; Tien, J. J Am Chem Soc 1998, 120, 8267.
10. Imhof, A.; Pine, D. J. Nature 1997, 389, 948.
11. Imhof, A.; Pine, D. J. Adv Mater 1998, 10, 697.
12. Takeichi, T.; Yamazaki, Y.; Zuo, M.; Ito, A.; Matsumoto, A.; Inagaki, M. Carbon 2001, 39, 257.
13. Kim, D. W.; Wang, S. S.; Hong, S. M.; Yoo, H. O.; Hong, S. P. Polymer 2001, 42, 83.
14. Hatori, H.; Kobayashi, T.; Hanzawa, Y.; Yamada, Y.; Iimura, Y.; Kimura, T.; Shiraishi, M. J Appl Polym Sci 2001, 79, 836.
15. Chen, X.; He, J.; Yan, C.; Tang, H. J Phys Chem B 2006, 110, 21684.
16. Puntes, V. F.; Krishnan, K. M.; Alivisatos, A. P. Science 2001, 291, 2115.
17. Sun, S.; Murray, C. B.; Weller, D.; Folks, L.; Moser, A. Science 2000, 287, 1989.
18. Nandi, M.; Conklin, J. A.; Salvati, L.; Sen, A. Chem Mater 1990, 2, 772.
19. Wozniak, M. E.; Sen, A.; Rheingold, A. L. Chem Mater 1992, 4, 753.
20. Bin, Y.; Oishi, K.; Koganemau, A.; Zhu, D.; Matsuo, M. Carbon 2005, 43, 1617.
21. Bin, Y.; Chen, Q.; Nakamura, Y.; Tsuda, K.; Matsuo, M. Carbon 2007, 45, 1330.
22. Geng, J.; Kinloch, I. A.; Singh, C.; Golovko, V. B.; Johnson, B. F. G.; Shaffer, M. S. P.; Li, Y.; Windle, A. H. J Phys Chem B 2005, 109, 16665.
23. Scheffler, M.; Greil, P.; Berger, A.; Pippel, E.; Woltersdorf, J. Mater Chem Phys 2004, 84, 131.
24. Luigi, N.; Gianfranco, C. Metal- Polymer Nanocomposites; Wiley: Hoboken, New Jersey, 2005.
25. Inagaki, M.; Morishita, T.; Kuno, A.; Kito, T.; Hirano, M.; Suwa, T.; Kusakawa, K. Carbon 2004, 42, 497.
26. Gay, F. P.; Berr, C. E. J Polym Sci Part A-1: Polym Chem 1968, 6, 1935.
27. Derbyshire, F. J.; Presland, A. E. B.; Trimm, D. L. Carbon 1975, 13, 111.
28. Oya, A.; Marsh, H. J Mater Sci 1982, 17, 309.
29. Lamber, R.; Jaeger, N.; Schulz-Ekloff, G. Surf Sci 1988, 197, 402.
30. Sing, K. S. W.; Everett, D. H.; Haul, R. A. W.; Moscou, L.; Pierotti, R. A.; Rouquerol, J.; Siemieniewska, T. Pure Appl Chem 1985, 57, 603.
31. Rouquerol, F.; Rouquerol, J.; Sing, K. Adsorption by Powders and Porous Solids: Principles, Methodology and Applications; Academic Press: London, 1999.
32. Kurk, M.; Jaroniec, M. Chem Mater 2001, 13, 3169.